

## COMMUNICATIONS

**A molecular picture of hydrophilic and hydrophobic interactions from *ab initio* density functional theory calculations**

Sheng Meng

*Department of Applied Physics, Chalmers University of Technology and Göteborg University, SE-412 96 Göteborg, Sweden and Institute of Physics, Chinese Academy of Sciences, P.O. Box 603, Beijing, 100080, China*

E. G. Wang

*Institute of Physics, Chinese Academy of Sciences, P.O. Box 603, Beijing 100080, China*

Shiwu Gao

*Department of Applied Physics, Chalmers University of Technology and Göteborg University, SE-412 96 Göteborg, Sweden*

(Received 14 April 2003; accepted 19 August 2003)

A molecular picture of hydrophilic and hydrophobic interactions, which ubiquitously exist in nature, has been proposed based on *ab initio* density functional study of water at two prototype metal (Pt and Au) surfaces. We demonstrate that the hydrophilicity–hydrophobicity can be characterized by the water–surface coupling and the strength of the hydrogen bond at the interfaces. From this picture, Pt is found to be hydrophilic while Au is hydrophobic, in agreement with experiment. The effect of the charge transfer and the long-ranged electron polarization of water on these interactions are also elaborated. © 2003 American Institute of Physics. [DOI: 10.1063/1.1617974]

The water–metal interface is full of rich structures and fascinating phenomena. One of the striking features is that different surfaces behave differently when they are in contact with water. Many surfaces like water, i.e., they are *hydrophilic*, while some others do not. They are thus *hydrophobic*. Classically, the concept of hydrophilicity–hydrophobicity was usually defined, on the macroscopic level, by the contact angle<sup>1</sup> (wetting angle) between water and the surface and applies essentially for liquid water.<sup>2</sup> However, recent experiments seem to suggest that this concept is applicable at the microscopic level and in the low temperature regime,<sup>3,4</sup> where wettability of a surface has been investigated by adsorption and desorption kinetics of water nanoclusters and thin ice films. In particular, it has been found in recent experiments<sup>5,6</sup> that the wetting order of several prototype substrates decreases as follows: Pt(111) > Ru(001) > Cs covered graphite > graphite > octane covered Pt(111) > Au(111). Despite the experimental indication, it is still unclear how to microscopically characterize the hydrophilic and hydrophobic interactions, especially on the molecular to electronic levels.

Here, we propose a molecular picture of hydrophilicity–hydrophobicity based on *ab initio* density functional theory (DFT) studies of water on Au(111) and Pt(111) surfaces. The surface electronic structure is shown to influence the hydrogen bond and the structure of water clusters and thin films through a localized charge transfer and a long-ranged electron polarization. From the analysis of the energetics of the interface water structures, we demonstrate that the hydrophilicity–hydrophobicity of the surfaces can be characterized by two quantities: the molecule–surface binding energy and the strength of the hydrogen bond at the interfaces.

This picture shows that Pt is hydrophilic while Au is hydrophobic, in agreement with experimental understandings. Our results establish the correlation between the electronic structures and the macroscopic properties of water–metal interfaces. Although demonstrated on two surfaces, our way for characterizing the hydrophilicity–hydrophobicity applies generally to other surfaces.

The calculation has been performed using the Vienna *ab initio* simulation program (VASP).<sup>7</sup> A supercell, which contains a 6(7)-layer slab of Pt (Au) atoms and a vacuum layer of 13 Å, was used to model the (111) surface with the calculated lattice constant of 3.99 Å for Pt and 4.18 Å for Au. Water molecules were put on one side (and both sides) of the slab. Plane waves cut off at 400 eV and a  $5 \times 5 \times 1$  or  $3 \times 3 \times 1$  k-point sampling have been used for the  $\sqrt{3} \times \sqrt{3} R30^\circ$  and  $3 \times 3 (2\sqrt{3} \times 2\sqrt{3} R30^\circ)$  supercells, respectively. This set of parameters assures energy convergence of 0.01 eV/atom. In structure optimization, the molecules and the first layer surface atoms were relaxed simultaneously with forces converged to 0.05 eV/Å. For the vibrational spectra, molecular dynamics (MD) simulations with 0.5 fs time step have been run for typically 2 ps at about 90 K after equilibrating the system for  $\sim 1$  ps. The Vanderbilt ultrasoft pseudopotentials<sup>8</sup> and the gradient-corrected exchange–correlation energy by Perdew and Wang (PW91)<sup>9</sup> were used.

Figure 1 shows schematically the adsorption geometry for different water clusters (a), bilayer (BL) (b), and a double bilayer (c) at the Au(111) surface (the cases for Pt look similar) obtained from the calculations. In order to examine different water states at the interface, both water clusters and extended thin films in a 2D hexagonal network as in ice Ih have been calculated. The size of the supercell were  $p(3 \times 3)$  for monomer, dimer and trimer,  $2\sqrt{3} \times 2\sqrt{3}$  for hexamer,

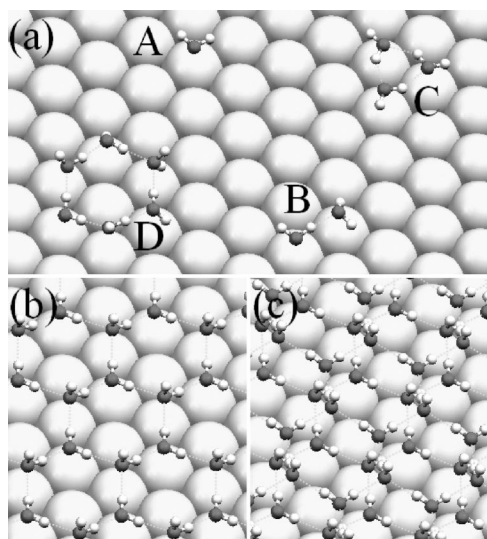


FIG. 1. The schematic geometries of (a) water monomer (A), dimer (B), trimer (C), hexamer (D), (b) bilayer, and (c) two bilayers adsorbed on Au(111) surface. The big white, black, and small white represent Au, O, and H atoms, respectively. The green lines indicate interwater hydrogen bonds. The structures for water/Pt(111) look similar.

and  $\sqrt{3} \times \sqrt{3}$  for the bilayer and multibilayers. The geometries of these small clusters look quite similar to their gas phase counterparts.<sup>10</sup> Water molecules prefer a top site adsorption, and tend to lie down onto the surface whenever possible. For example, both the donor and acceptor molecule of the dimer take a top site as shown in Fig. 1(a) case B, although the donor couples stronger to the surface than the acceptor, forming two metal–water (M–H<sub>2</sub>O) bonds plus an internal hydrogen bond (H-bond) (see Table I). Trimer and hexamer remain their ringlike structure and lie flatly on the surface, as shown in Fig. 1(a). The trimer thus makes 3 M–H<sub>2</sub>O bonds and 3 H-bonds, while the hexamer has 3 M–H<sub>2</sub>O bonds and 6 H-bonds. Similar counting rules apply for bilayers and multibilayers. In thin films, water form extended 2D networks, as in bulk ice<sup>11</sup> with a  $\sqrt{3} \times \sqrt{3}$  R30° pattern, as found both experimentally<sup>3,4</sup> and from the *ab initio* DFT calculation.<sup>12,13</sup> In bilayer and multibilayers, only molecules in the bottom form M–H<sub>2</sub>O bond (see Fig. 1). The M–H<sub>2</sub>O bond length

TABLE II. Calculated and experimental vibrational energies for the ice bilayer on Pt(111) and Au(111) (in meV). See Refs. 18 and 19 for experimental data and the assignment of these modes. Value in parentheses is taken from water/Ag(111) (Ref. 20).

Substrate		Translations and librations					$\delta_{\text{HOH}}$	$\nu_{\text{O-HB}}$	$\nu_{\text{O-H}}$
Pt	Theo.	18	32	53	69	87	198	388, 432	467
	Expt.	16.5	33	54	65	84	201	424	455
Au	Theo.	17	36			108	201	400 444	455
	Expt.		31			104	205	409	(452)

varies between 2.3 Å, for the bottom water, and 3.4 Å, for water in the upper layer. Another adstructure, the  $\sqrt{39} \times \sqrt{39}$  R16.1° phase,<sup>14,15</sup> is also calculated. It exhibits similar atomic arrangement as that in  $\sqrt{3} \times \sqrt{3}$  bilayer. The detailed structure and bonding information for all the calculated cases are summarized in Table I.

The energetics of the interface water are also given in Table I, where the adsorption energy,  $E_{\text{ads}}$ , has been defined as the averaged adsorption energy per molecule,

$$E_{\text{ads}} = (E_{\text{Metal}} + n \times E_{\text{H}_2\text{O}} - E_{(\text{H}_2\text{O})_n/\text{Metal}}) / n. \quad (1)$$

Here  $E_{(\text{H}_2\text{O})_n/\text{Metal}}$  is the total energy of the adsorption system,  $E_{\text{Metal}}$  and  $E_{\text{H}_2\text{O}}$  are those for the surface and free molecules, respectively, and  $n$  is the number of water in the unit cell. Two features are clearly seen from the energetics: (i) The  $E_{\text{ads}}$  for monomer on Pt(111), 304 meV, is almost three times of that on Au(111), 105 meV, suggesting a much stronger water–metal interaction on the Pt surface compared to Au. Similar energy difference, 50–200 meV, exists for all other structures studied; and (ii) the energy oscillates significantly for the small clusters, due to the dramatic change in the structure and coordination number, while it increases gradually in thin films, from bilayer to up to six bilayers. Among the small clusters investigated, the water hexamer is most stable, supporting the experimental findings that water hexamers were observable in the scanning tunneling microscopy.<sup>16,17</sup> To justify these structures, the vibrational spectra were calculated for vibrational recognition.<sup>13</sup> The eigenfrequencies for the bilayer, shown in Table II for example, compare favorably with the available experimental

TABLE I. The structure and energetics for water clusters and thin films on the Pt(111) and Au(111). The unit cell, the number of molecules ( $n$ ), the number of metal–OH<sub>2</sub> bonds,  $N_{\text{M-H}_2\text{O}}$ , and the number of H-bonds,  $N_{\text{HB}}$ , in the unit cell are shown together with the adsorption energies ( $E_{\text{ads}}$ ) and the H-bond energies ( $E_{\text{HB}}$ ) (in meV). The two energies for the bilayer correspond to the H-up/H-down cases (Ref. 13).

Ads. species	Unit cell	$n$	$E_{\text{ads}}(\text{Pt})$	$E_{\text{ads}}(\text{Au})$	$N_{\text{M-H}_2\text{O}}$	$N_{\text{HB}}$	$E_{\text{HB}}(\text{Pt})$	$E_{\text{HB}}(\text{Au})$
Monomer	$3 \times 3$	1	304	105	1	0	-	-
Dimer	$3 \times 3$	2	433	259	2	1	258	308
Trimer	$3 \times 3$	3	359	283	3	3	55	178
Hexamer	$2\sqrt{3} \times 2\sqrt{3}$	6	520	402	3	6	368	350
Bilayer	$\sqrt{3} \times \sqrt{3}$	2	505/527	437/454	1	3	235	256
2 bilayers	$\sqrt{3} \times \sqrt{3}$	4	564	489	1	7	312	271
3 bilayers	$\sqrt{3} \times \sqrt{3}$	6	579	508	1	11	303	272
4 bilayers	$\sqrt{3} \times \sqrt{3}$	8	588	520	1	15	307	279
5 bilayers	$\sqrt{3} \times \sqrt{3}$	10	593	532	1	19	307	290
6 bilayers	$\sqrt{3} \times \sqrt{3}$	12	601	545	1	23	320	305
Bilayer	$\sqrt{39} \times \sqrt{39}$	32	615	-	16	48	309	-
2 bilayers	$\sqrt{39} \times \sqrt{39}$	64	582	-	16	112	275	-
3 bilayers	$\sqrt{39} \times \sqrt{39}$	96	572	-	16	176	276	-

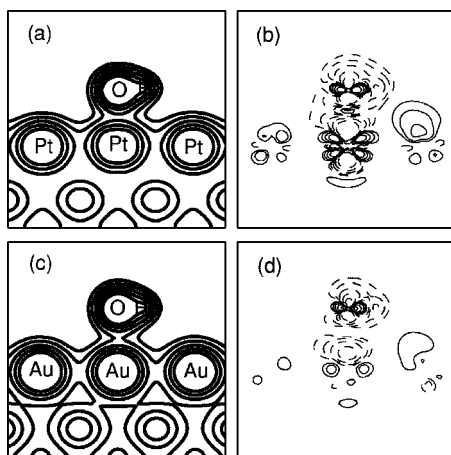


FIG. 2. The isodensity contours for the total and difference electron density for water monomer on Pt, panels (a) and (b), and Au, (c) and (d). The difference density was defined as  $\Delta\rho = \rho[\text{H}_2\text{O}/\text{Metal}] - \rho[\text{Metal}] - \rho[\text{H}_2\text{O}]$ . The contours have densities  $\rho = 0.1 \times 2^n e/\text{\AA}^3$  and  $\Delta\rho = \pm 0.005 \times 2^n e/\text{\AA}^3$ , for  $n=0-4$ . Solid and dashed lines correspond to  $\Delta\rho > 0$  and  $\Delta\rho < 0$ , respectively.

data.<sup>18,19</sup> Estimated from vibrational spectra, the zero-point energy is  $\sim 90$  meV per molecule for the first bilayer, which stabilize the adlayer by 30 meV relative to ice Ih. Although the  $\sqrt{39} \times \sqrt{39}$  phase has a slightly larger adsorption energy at the first bilayer, it is found to transform into  $\sqrt{3} \times \sqrt{3}$ , as the coverage increases to three bilayers, in agreement with recent experiment.<sup>15</sup> For a direct comparison with water/Au, we thus focus on the  $\sqrt{3} \times \sqrt{3}$  structure hereafter.

The difference in the energetics between Pt and Au has its origin in the electronic structure. Figure 2 shows the isodensity contours of the total and induced electron density for water monomer adsorbed on Pt(111) [panels (a) and (b)] and Au(111) [(c) and (d)]. The horizontal axis is in the [110] direction, and also goes approximately along one of the OH bonds, while the vertical axis is in the surface normal. The induced density differs dramatically with a  $d_{z^2}$  character on Pt (b) but an  $s+p_z$  character on the Au (d) surface. There is more charge transfer on Pt(111) compared to Au(111). This result is not surprising because Au has filled  $d$ -bands, which are 3–10 eV below the Fermi level, while there are abundant surface states of  $d_{xz}$  and  $d_{z^2}$  character near the Fermi level on Pt(111). The fundamental difference between Pt and Au results from the presence (on Pt)/absence (on Au) of  $d$ -band in participating the interaction upon water adsorption. This conclusion is consistent with earlier studies<sup>20,21</sup> of water adsorption on other surfaces, where the  $d_{z^2}$ -lone pair coupling was found to be crucial for the molecule–surface interaction. For the clusters and thin films, such a picture also applies, because the coupling occurs mainly through the bottom molecule, whose interaction is very similar to the monomer case. Figure 3 shows the 2D induced charge density for five bilayers adsorbed on Au and Pt and their planar average along the surface normal. In addition to the charge transfer localized at the interfaces, a long-range electron polarization of the water films can clearly be seen. This long-range polarization was mainly induced by the surface potential at the interfaces.

Now we turn to discuss the wettability of a surface from the viewpoint of energetics. Generally speaking, the wetta-

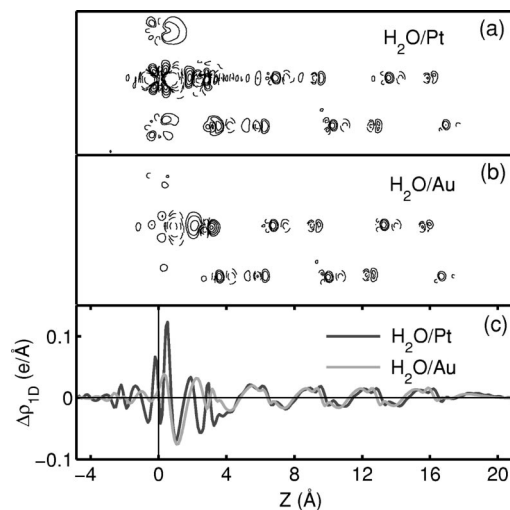


FIG. 3. The induced charge density, with the same values as in Fig. 2, for thin film water of five bilayers on Pt(111) (a) and Au(111) (b). Panel (c) shows the planar average of the induced density along the surface normal.

bility of a surface, exhibited by macroscopic water structures, is essentially determined by two energetic parameters at the microscopic scale, namely the surface–water coupling and the strength of H-bond. These two parameters determine the configuration preference and the stability of a water structure at the interfaces, namely, whether a structure with more H-bonds or with more metal–surface bonds is preferred and energetically stable. A surface with stronger metal–surface bond, compared to the H-bonding, would favor adsorption on the metal surface, rather than on water, and would eventually behave hydrophilic. A surface with weaker surface–water coupling should be hydrophobic. Unfortunately, these two interactions are strongly hybridized with each other in the structures studied in Fig. 1 both electronically and energetically, as shown by the  $E_{\text{ads}}$  defined in Eq. (1). Moreover, the variation of  $E_{\text{ads}}$  in Table I reflects mainly the change in the number of bonds and coordinations rather than the strength of the two interactions, and cannot be used directly to interpret the hydrophobicity–hydrophilicity of the surfaces. To separate the two interactions, we introduce the following way to extract the strength of the H-bond,  $E_{\text{HB}}$ , in the adsorbed water structures,

$$E_{\text{HB}} = \begin{cases} (E_{\text{ads}} \times n - E_{\text{ads}}[\text{monomer}] \times N_{\text{M-H}_2\text{O}}) / N_{\text{HB}}, & \text{for clusters and 1 BL} \\ (E_{\text{ads}}[m \text{ BL}] \times 2m - E_{\text{ads}}[(m-1)\text{BL}] \times 2(m-1)) / 4, & \text{for } m \text{ BL, } m > 1. \end{cases} \quad (2)$$

Here  $E_{\text{ads}}[\text{monomer}]$  and  $N_{\text{M-H}_2\text{O}}$  are the adsorption energy of monomer and the number of molecule–surface bonds in the water structures; and  $E_{\text{ads}}[m \text{ BL}]$  is the adsorption energy for  $m$  bilayers. Water monomer binding energy has been utilized as universal parameter here, because it also gives a good representation of water–metal coupling in bilayer and clusters.<sup>22</sup> The  $E_{\text{HB}}$  introduced this way characterizes the mean H-bond energy in a cluster. For multibilayers,  $E_{\text{HB}}$  reflects the mean strength of the four H-bonds in the outermost bilayer.

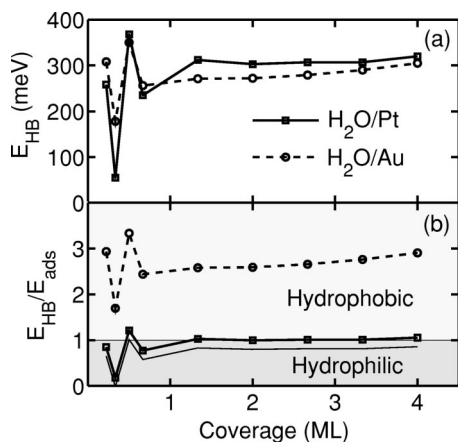


FIG. 4. (a) The H-bond energy,  $E_{HB}$ , and (b) the wettability, defined as  $w = E_{HB}/E_{ads}$ , as a function of coverage for various water clusters and thin films on Pt and Au surfaces. Here 1 ML is defined as a  $p(1 \times 1)$  surface structure of the (111) surface of Au and Pt. One has to multiply the ML by a factor 3/2 to get the coverage in water bilayers, and by 3 for the coverage in water layers. When taking into account the zero-point energy correction of the H-bond, the  $H_2O/Pt$  curve shifts downward to the thin solid line in (b).

The obtained  $E_{HB}$  in Table I has been plotted in Fig. 4(a) as a function of coverage. The latter was simply defined as the number of molecules divided by the size of the surface cell. Note that the coverage for clusters can only be viewed as pictorial rather than physically accurate, as the calculations were done to model isolated clusters at zero coverage. This however does not affect the physics of the following discussion. The H-bond energy in Fig. 4(a) changes substantially from dimer (2/9 ML) to trimer (1/3 ML) and hexamer (1/2 ML), due to dramatic change in orientation and coordinations in the clusters. From bilayer to 6 bilayers, the H-bond energy increases gradually and reaches 320 meV (Pt) and 305 meV (Au), which are comparable to the experimental data for ice Ih, 315 meV (including zero-point energy),<sup>12</sup> suggesting that the effect of the metal substrates becomes small beyond this coverage. Comparing Figs. 4(a) and 3, we see a close correlation between the energetics of the H-bond and electronic structure at the interfaces. The localized charge transfer on Pt leads to a sudden jump in  $E_{HB}$  at 4/3 ML (2 bilayers) and a relatively flat region from two to six bilayers. While on Au the long-range electron polarization becomes more important due to the smaller charge transfer, leading to a gradual increase of the H-bond energy (from 2/3 to 4 ML) and the much longer distance dependence in Fig. 4(a). At six bilayers, the H-bond on Au is still lower than that on Pt. This indicates that the polarization interaction might not be negligible even beyond this coverage. Lattice mismatch between the surface and the bulk ice might also be responsible for this difference. The 2D lattice constants are 2.61 Å for ice Ih, 2.82 Å for the bilayer on Pt(111) (8% mismatch), and 2.95 Å for that on Au(111) (13% mismatch). The better fit on Pt(111) may yield slightly larger energy of the H-bond.

Figure 4(b) shows the ratio between the H-bond energy and the adsorption energy (for monomer<sup>22</sup>),  $w = E_{HB}/E_{ads}$ , a quantity characterizing the wettability of a surface. *Qualita-*

*tively*, we may take  $w=1$  as roughly the border between hydrophilic and hydrophobic interactions. (Such a division at  $w=1$  should only be considered as approximate.) Although the two curves oscillate in the cluster region, the water/Au case (dashed line) lies up in the  $w \gg 1$  region, demonstrating that Au is hydrophobic. On the contrary, water/Pt (solid line) is in the hydrophilic,  $w \leq 1$ , region. This difference results essentially from the much stronger water–Pt interaction, giving a three times larger adsorption energy on Pt compared to that on Au surface. A general implication of this result is, as we believe, that the hydrophilicity–hydrophobicity is directly correlated to the monomer adsorption energy on different surfaces.<sup>23</sup> If the zero-point energy of the H-bond is corrected (ZPEC) by subtracting that of ice Ih, 60 meV,<sup>12</sup> the water/Pt case will be shifted down to the thin solid line in Fig. 4(b), lying completely in the  $w < 1$  region. (The ZPEC to water/Au is small.) The large gap between the two curves indicates the great difference in wettability of Pt and Au. Such an analysis, though carried out here on two specific surfaces, should be generally applicable to other systems.<sup>23,24</sup>

This work was supported by The Swedish Research Council (VR) through VR 621-2001-2614, the Natural Science Foundation of China, and the National Key Project for Basic Research (G2000067103). The authors thank HPC2N, the High Performance Computer Center at North, Sweden, for allocated computer time.

- <sup>1</sup>P. G. de Gennes, *Rev. Mod. Phys.* **57**, 827 (1985).
- <sup>2</sup>T. Hayashi, A. J. Pertsin, and M. Grunze, *J. Chem. Phys.* **117**, 6271 (2002).
- <sup>3</sup>A. Thiel and T. E. Madey, *Surf. Sci. Rep.* **7**, 211 (1987).
- <sup>4</sup>M. A. Henderson, *Surf. Sci. Rep.* **46**, 1 (2002).
- <sup>5</sup>R. S. Smith, C. Huang, E. K. L. Wong, and B. D. Kay, *Surf. Sci.* **367**, L13 (1996).
- <sup>6</sup>P. Löfgren *et al.*, *Surf. Sci.* **367**, L19 (1996).
- <sup>7</sup>G. Kresse and J. Hafner, *Phys. Rev. B* **47**, 558 (1993); **49**, 14251 (1994); *J. Phys.: Condens. Matter* **6**, 8245 (1994).
- <sup>8</sup>D. Vanderbilt, *Phys. Rev. B* **41**, 7892 (1990).
- <sup>9</sup>J. P. Perdew *et al.*, *Phys. Rev. B* **46**, 6671 (1992).
- <sup>10</sup>J. K. Gregory *et al.*, *Science* **275**, 814 (1997).
- <sup>11</sup>D. L. Doering and T. E. Madey, *Surf. Sci.* **123**, 305 (1982).
- <sup>12</sup>P. J. Feibelman, *Science* **295**, 99 (2002); D. Menzel, *ibid.* **295**, 58 (2002).
- <sup>13</sup>S. Meng, L. F. Xu, E. G. Wang, and S. W. Gao, *Phys. Rev. Lett.* **89**, 176104 (2002).
- <sup>14</sup>A. Glebov, A. P. Graham, A. Menzel, and J. P. Toennies, *J. Chem. Phys.* **106**, 9382 (1997).
- <sup>15</sup>S. Haq, J. Harnett, and A. Hodgson, *Surf. Sci.* **505**, 171 (2002).
- <sup>16</sup>K. Morgenstern and J. Nieminen, *Phys. Rev. Lett.* **88**, 066102 (2002).
- <sup>17</sup>T. Mitsui *et al.*, *Science* **297**, 1850 (2002).
- <sup>18</sup>K. Jacobi, K. Bedürftig, Y. Wang, and G. Ertl, *Surf. Sci.* **472**, 9 (2001).
- <sup>19</sup>G. Pirug and H. P. Bonzel, *Surf. Sci.* **405**, 87 (1998).
- <sup>20</sup>A. F. Carley, P. R. Davies, M. W. Roberts, and K. K. Thomas, *Surf. Sci.* **238**, L467 (1990).
- <sup>21</sup>H. P. Bonzel, G. Pirug, and J. E. Müller, *Phys. Rev. Lett.* **58**, 2138 (1987).
- <sup>22</sup>This is justifiable if we keep one water fixed and remove the other one from the bilayer configuration (thus no hydrogen bonding), the sum of adsorption energy for the two separate water molecules is 270 meV (H-up) and 340 meV (H-down), very close to one monomer adsorption energy, 304 meV. This is also approximately true for dimer adsorption.
- <sup>23</sup>It is worth mentioning that a linear correlation between the contact angle and the monomer adsorption energy has been demonstrated explicitly (see Ref. 24) in a model description of water on graphite surface.
- <sup>24</sup>T. Werder, J. H. Walther, R. L. Jaffe, T. Halicioglu, and P. Koumoutsakos, *J. Phys. Chem. B* **107**, 1345 (2003).